

REVIEWS OF TOPICAL PROBLEMS

PACS numbers: **02.30.–f, 42.90.+m**

Microscopy of subwavelength structures

V P Tychinskiĭ

Contents

Abstract. **A more accurate formulation of the Abbe theory is presented using well-known open resonator results, namely, field representation in terms of the eigenfunctions of the optical system viewed as a segment of an equivalent lens waveguide; and the use of the mirror Fresnel number dependence of the diffraction losses of high-order Gaussian beams for describing the image distortions due to the objective aperture. The number of the degrees of freedom of the image within the zero mode waist area is estimated by using the Hermite-Gaussian functions within the paraxial approximation framework.**

1. Introduction

If the superresolution provides an opportunity of seeing the invisible, is the very idea of its realization not in conflict with everyday experience? Indeed, the diffraction image of a point in an optical system has a finite size, and any attempt to distinguish details inside the diffraction spot has, at first glance, no sense.

Nevertheless, the number of reports on superresolution grows increasingly and reveals some clear-cut trends in research that suggest the positive answer to the above question:

(1) algorithmic, aiming at the reconstruction of an object based on diffraction-limited or distorted primary information

(2) heuristic, related to new ideas and instrumental techniques intended to overcome the diffraction limit (near-field, confocal microscopy)

(3) informative, based on the use of up-to-date tools and devices in conventional optical systems (contrast enhancement, computer-assisted phase-contrast microscopy).

The present communication does not pretend to be a comprehensive review of the superresolution problem on the whole and will be restricted to an analysis of recent data obtained in the framework of the latter approach. Here is a brief review of key previous publications.

The use of TV techniques for contrast enhancement in microscopy has been discussed in the literature since 1951. Allen et al. [1] and Weiss et al. [2] reported on further developments of this approach including microscopic observations of unambiguously identified extended biological objects and organelles with transverse sizes of down to $d = 10$ nm using high-magnifying oil-immersion objectives in conjunction with differential, interferential, and polarizing contrast enhancement.

This corresponds to the normalized superresolution $S = d_R/d = 20$ for an objective with numerical aperture $NA = 1.3$. Here, $d_R = 0.61\lambda F/a$ is the Rayleigh radius (the classical resolution limit), F is the focal length, and a is the aperture radius. A detailed description of the contrast enhancement can be found in a book by S Inoue [3].

The above findings demonstrated the possibility of achieving, in principle, superresolution in conventional amplitude images and were confirmed in a series of subsequent studies and in phase-contrast images obtained under coherent illumination using a computer-aided Airyscan microscope [4 – 6].

An important feature of the experiments reported by Allen and other authors was the fact that the superresolution was obtained with conventional microscopes using phase-contrast and polarization techniques in conjunction with analog video devices. This was achieved by the background subtraction, a proper choice of the illumination conditions and compensator and analyzer positions, etc. The conditions for contrast enhancement were virtually reduced to the extension of the dynamic range of brightness of the image when examining anisotropic biological objects in a field with a phase gradient.

Those works ignored the obvious discrepancy between the experimental results and the classical diffraction theory of optical systems [7, 8] and assumed the enhanced resolution to be related to the substitution of the Rayleigh criterion with Sparrow's limit. Also, it was supposed that the image shape and size inside the Airy disk might be distorted, minor details disappeared, etc.

Naturally, reports on superresolution gave impetus to basic research in this field. In 1952, Toraldo di Francia [9] suggested the possibility of restoring object's details beyond

V P Tychinskiĭ Moscow State Institute for Radioengineering, Electronics and Automation, Vernadskiĭ prosp. 78, 117454 Moscow, Russia
Tel. (7-095) 434-67 92. Fax (7-095) 434-86 65
E-mail: vladimir@tych.pvt.msu.su

Received 7 March 1996, revised 17 June 1996
Uspekhi Fizicheskikh Nauk **166** (11) 1219–1229 (1996)
Translated by Yu V Morozov, edited by S N Gorin

the diffraction limit. A comprehensive analysis of later studies is outside the scope of the present communication (they are briefly reviewed in [10]), but it seems appropriate to emphasize the explanation by Pask [11] of the passage through an aperture of information on the Fourier component of the angular spectrum that is outside the numerical aperture of the objective.

With the field of view of an objective being limited, the diffraction maximum width may prove large enough to allow a substantial portion of scattered radiation energy to pass through the aperture even if the diffraction angle of the central component is larger than the aperture angle. Note that the author implicitly assumed the existence of the scattering function and the location of the aperture in the far field. However, this line of reasoning does not lead to the understanding of the presence of image elements whose size is significantly smaller than the wavelength and which are formally associated with evanescent waves.

We suggested a different model to explain the superresolution in phase-contrast images based on the properties of wave-front dislocations and Hermite-Gaussian functions which are eigenfunctions of axially symmetrical optical systems [12].

This model represents the object's field as the sum of two modes $TEM_{0,0}$ and $TEM_{0,2}$. The distance d between the zero-intensity lines (hereinafter to be called merely zero-lines) for a certain amplitude ratio may be significantly smaller than the waist radius w_0. At the zero-lines, phase changes by 180° (π-jumps) occur, which, at a sufficiently large magnification, may be located in the image plane. The field amplitude at intermediate points between zero-lines decreases with the squared distance d, which allowed a simple energy-dependent resolution criterion $d/w_0 = (S/N)^{-1/2}$ to be obtained, where S/N is the signal-to-noise ratio. Also, the study has shown that the action of a finite aperture disturbs the amplitude–phase relationship between the modes in the image plane and results in systematic errors in the location of zero-lines. Assuming that the zero-lines of the field correspond to the boundaries of an abstract structural element at the object's surface, minimum information on the boundaries of subwavelength structures can be obtained with a very small number of modes in the object's field [12]. However, the cited work did not examine the superresolution in amplitude images, nor did it use the image representation inside the Airy disk as functions of the degrees of freedom of the field, or attempt to numerically estimate the maximum resolving power.

A common problem in all microscopic studies is the evaluation of qualitative and quantitative correspondence between an object and its image. Its importance is even greater as regards the superresolution, which is confirmed by the results of near-field microscopy [13 – 15].

The application of phase-contrast microscopy and profile measurements [16 – 18] traditionally implies determination of the equivalent height function $h(r)$ related to the physical parameters of the surface and to the 'field portrait'. In the simplest case, it is proportional to the reflected-wave phase. However, the local value of this phase in the case of inhomogeneous, anisotropic, and transparent stratified structures does not provide information about the real surface of an object as caused by its physical parameters [7, 8] but represents the phase of the 'field portrait'. An even more complicated dependence of these functions arises when the size of structural elements is comparable with the wavelength and also if the polarization of the incident light is taken into account. Indeed, in the theory of optical systems, an object is given by a complex function of coordinates at the plane of field representation, and the complete correspondence of such a 'field portrait' with the real physical object is far from being evident. Few analytical solutions available from the diffraction theory suggest that the 'portrait' depends on local impedance values, incident wave polarization, and other factors. Therefore, *a priori* information is sometimes necessary or at least desirable to correctly interpret images obtained (especially subwavelength images).

Numerical field calculations in the scalar approximation [8, 19, 20] entail marked inaccuracy already at the normalized sizes of structural elements at the object's surface such as $d/\lambda \geqslant 20$; labor-consuming analytical solutions of the stringent diffraction theory and numerical calculations are available for a very small number of models [8, 20]. Direct measurements with the use of 'near-field' microscopy [13 – 15] in the optical frequency range yield conflicting results and fail to provide quantitative characteristics for complex fields, which hampers the real possibility of obtaining the 'field portrait' of an object, while simulation of optical images in the microwave range [21, 22] requires a number of assumptions and poses certain experimental problems.

Measurements with a coherent-probe microscope [23, 24] have also demonstrated the disturbed linear relationship between a subwavelength object and its phase image because of diffraction at the aperture at small d/λ. Therefore, one has for the time being to reconcile oneself with the lack of a simple algorithm for the evaluation of the correspondence between a real subwavelength structure and its field portrait.

Probing measurements of the near-field phase and amplitude by M Totzeck using dielectric models in the microwave frequency range [21, 22] appear to be of special interest since they demonstrated the possibility of identifying structures with linear size as small as 0.03λ in the 'field portrait,' to evaluate the correspondence between an object and its 'portrait' in some specific cases and the effect of a finite aperture.

Ref. [22] also reported results of computer simulation of transferring the field portrait of a phase object by an optical system. As usual, the action of the entrance aperture was identified with that of a low-pass filter. The author concluded, based on the results of calculations [22], that a major portion of the initial information was lost at the aperture, and the likeness between the image and the object could be obtained only if the following conditions were satisfied:

(1) There is marked phase contrast at the boundaries of structural elements (the difference between diffracted wave phases on either side of the boundary close to π);

(2) For structural elements in the form of an extended slit, its width is not less than $0.25\,\lambda$;

(3) Images are interrelated in terms of polarization. The difference between objects and their phase images increases with decreasing d/λ ratio. It is calculated that the slit width in the image significantly exceeds the real value already at $d/\lambda = 0.4$.

Thus, it may be inferred from [21, 22] that although plausible information on an object exists in the amplitude and phase of the near field for objects's sizes as small as $d/\lambda = 0.03$, in the image phase such information is only available at $d/\lambda \geqslant 0.25$. This is equivalent to the assertion that the superresolution coefficient S (an excess over the Rayleigh criterion) in phase images is not greater than 2.

This conclusion seems natural because, to our knowledge, all studies concerned with the theory of optical systems ignored energy-related aspects and identified diffraction at the aperture with the cut-off of higher spatial frequencies, which inevitably led to the classical resolution criterion and was at variance with experimental findings.

It follows from this brief review of superresolution studies that a few problems of different levels should be specified and considered separately:

(1) Physical and theoretical explanation of the essence of the phenomenon, evaluation of the role of energy relationships, consensus of concepts, terminology, models, and resolution criteria;

(2) Elaboration of the consistent theory of superresolution;

(3) Determination of a 'field portrait' in the basis of optical system eigenfunctions and criteria for the correspondence between a real physical object and its 'field portrait,' with due regard for the specificity of functional images (phase, polarization, gradient, etc);

(4) Analysis of adequate technical tools for the realization of superresolution in various functional images;

(5) Comparison of experimental findings and key theoretical data.

At present, we have no acceptable explanation for the available experimental findings. The further discussion concerns feasible models and approaches to the solution of the superresolution problem with special emphasis on the physical nature of the phenomenon of interest, requisites for the development of a strict theory, new results of subwavelength structure measurements with a computer-aided phase-contrast microscope, and qualitative comparison of known experimental findings and data ensuing from the proposed physical concept.

2. The theoretical model

The theory of optical systems [8] considers an object expanded in either plane waves or eigenfunctions of an optical system. These functions are in fact solutions of the Fredholm integral equation with a symmetric kernel and may be represented as the product of two functions of the transverse coordinates x, y. For an arbitrary function $o(x_0, y_0)$, e.g., for the field of an object in the $\Phi_{n,m}$ basis, the amplitudes $O_{n,m}$ can be defined as

$$o(x_0, y_0) = \sum_{n,m=0}^{\infty} O_{n,m} \Phi_n(x_0)\, \Phi_m(y_0)\,. \tag{1}$$

The works of Toraldo di Francia, Landau, and Pollack reviewed in [8] demonstrated that solutions for eigenfunctions $\Phi_n(x_0)$, $\Phi_m(y_0)$ for a small field of an object of size L have the form analogous to angular spheroidal functions with a limited range of eigenvalues $\gamma_{n,m}$, and the image field may be represented by a finite sum

$$\begin{aligned}\mathbf{E}(x, y) &= \sum_{n,m=0}^{\infty} \gamma_n \gamma_m O_{n,m} \Phi(x)\, \Phi_m(y) \\ &\cong \sum_{n,m=0}^{q} \gamma_n \gamma_m O_{n,m} \Phi_n(x)\, \Phi_m(y)\,. \end{aligned} \tag{2a}$$

The finite number of terms in (2a) is due to the fact that moduli of eigenvalues $\gamma_{n,m}$ decrease sharply at

$$n, m \leqslant q = \frac{La}{\lambda F}\,, \tag{2b}$$

which leads to loss of information contained in the remaining terms of the sum.

The series (2a) may be interpreted [8] as the expansion of function $\mathbf{E}(x, y)$ into its constituent components in infinite-dimensional Gilbert space, in which the functions $\Phi_{n,m}$ form the basis. Each term of the series is actually one degree of freedom of the image field. The filtering effect of the aperture manifests itself in the limitation on the range of eigenvalues $\gamma_{n,m}$.

This result makes it possible to approach the superresolution problem from a different standpoint, which implies the calculation of additional or 'internal' degrees of freedom inside the Airy disk.

The present report provides an opportunity to further elaborate the approach to the physical interpretation of the observed superresolution first initiated in [12]; also, we will use the aforementioned fruitful concepts of the eigenfunctions of an optical system and the degrees of freedom of an image to prove the possibility, in principle, of increasing the number of degrees of freedom in excess of the (2b) limit.

In order to determine eigenfunctions of an optical system, let us consider the simplified optical scheme of a microscope shown in Fig. 1, where a flat mirror is placed in the focal plane $z = 0$ and illuminated through lens l_1 by a Gaussian beam of the zeroth mode $TEM_{0,0}$ with waist radii w_0 and W_0 in the planes of the object and the lens, respectively. The reflected beam passes through the lens in the backward direction and has a waist radius W_i in the image plane z_i. The optical equivalent of the scheme presented in Fig. 1 is an open resonator or a fragment of a lens waveguide in Fig. 1b. The eigenfunctions of optical resonators have been described in great detail [8, 25–28]; for stable configurations in the paraxial approximation, they are in fact the complete orthonormalized set of the Hermite-Gaussian or Laguerre-Gaussian modes with two integer-valued indices n, m and p, l for the Cartesian and polar coordinate systems, respectively:

$$\begin{aligned} U_{n,m} &\cong H_n\left(\sqrt{2}\frac{x}{w}\right) H_m\left(\sqrt{2}\frac{y}{w}\right) \exp\left(-\frac{\rho^2}{w^2}\right), \\ U_{p,l} &\cong L_p^l\left(2\frac{\rho^2}{w^2}\right) \begin{Bmatrix} \sin l\phi \\ \cos l\phi \end{Bmatrix} \exp\left(-\frac{\rho^2}{w^2}\right), \end{aligned} \tag{3}$$

where $H_{n,m}$ and L_p^l are the Hermite and Laguerre polynomials, respectively.

The paraxiality condition is equivalent to the fulfillment of the inequality $\lambda^2/2\pi^2 w_0^2 \ll 1$ or the assumption that the characteristic scale of field changes $d_{x,y}$ satisfies the condition

$$\frac{k d_{x,y}^2}{2z} \gg \pi\,. \tag{4}$$

It was shown [26] that neglecting third-order terms in the phase multiplier of the diffraction integral for the computation of the field in a confocal resonator is equivalent to the restriction of the Fresnel numbers

$$N_F \ll (NA)^2\,. \tag{5}$$

The estimates below indicate that inequalities (4) and (5) are not fulfilled under real conditions; hence, functions (3) are not exact solutions for an optical system with large Fresnel

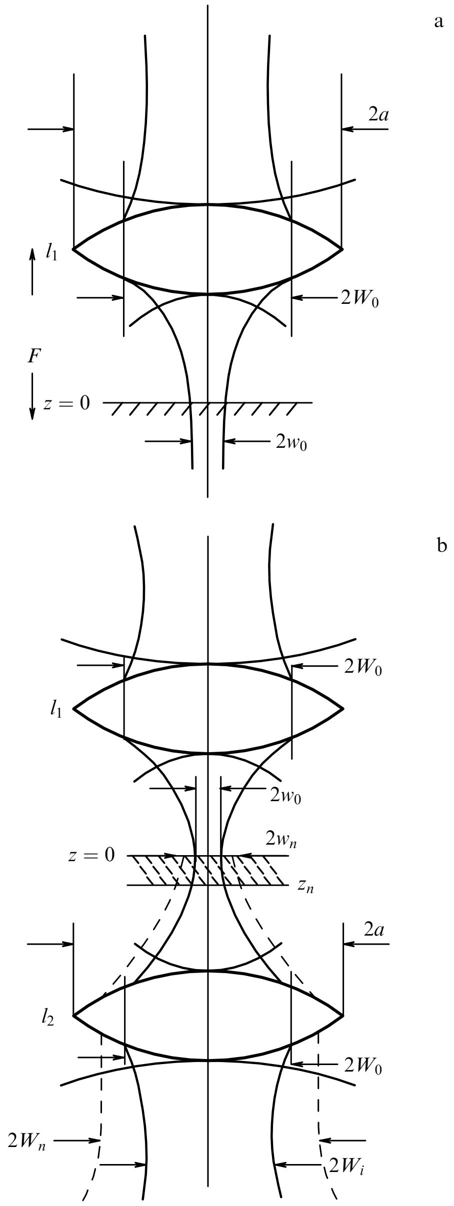

Figure 1. (a) Simplified optical arrangement of a microscope: l_1 is the objective; F is the flat mirror located in the focal plane $z=0$; w_0 and W_0 are the waist radii of the zeroth modes in the plane of the object and lens, respectively; and a is the aperture radius. (b) Fragment of a lens waveguide (optical equivalent of the scheme in Fig. 1a): w_n and W_n are the radii of the nth mode; $W_{\rm i}$ is the zero-mode waist radius in the image plane; and z_n is the boundary of the near field, in which the amplitude of the nth mode decreases exponentially.

numbers. Nevertheless, we will consider (3) as the basis, assuming that the use of more accurate solutions, e.g., in the form of spheroidal or ellipsoidal functions [8], is unlikely to substantially affect the results.

Now, let us turn again to Fig. 1b and suggest that a dephasing transparency with transfer function $T(x_0,\ y_0)$ is placed in the focal plane $z=0$; it has no effect on the basis (3) and functions solely as a spatial modulator.

The field $E_0(x,y,0)=T(x_0,\ y_0)\,e(x,y)$ due to the currents induced at the transparency surface and the field $e(x,\ y)$ of an incident wave within a limited region satisfy the boundary conditions in the equivalent plane of the representation $z=0$. In the general case, the field $E_0(x,y,0)$ can have local components with a spatial scale of changes $d \ll \lambda$ and can serve as a source of scattered waves in the form of higher-order Gaussian beams.

Let $w_{n,m}$ and $W_{n,m}$ be the radii of the corresponding modes in the plane $z=0$ and in the plane of lens l_2. Bearing in mind the remarks made above, the eigenfunctions of the lens waveguide fragment and the equivalent open resonator with the transfer function $T(x,y)$ are represented by a set of Hermite-Gaussian functions

$$U_{n,m}(x,y,z)=\frac{C_{n,m}}{(1+z^2/b^2)^{1/2}}\,\Phi_n\left(\frac{\sqrt{2}x}{w}\right)\Phi_m\left(\frac{\sqrt{2}y}{w}\right)\times\exp\left[-\frac{\mathrm{j}k}{2R}(x^2+y^2)\right]\exp\left[\mathrm{j}(m+n+1)\,\phi\right], \qquad (6)$$

where

$$C_{n,m}=\left(\frac{2}{w_0^2\pi 2^{m+n}m!n!}\right)^{1/2}, \quad \phi=\arctan\frac{z}{b}, \quad w_0=\sqrt{\frac{2b}{k}}, \qquad (7)$$

with b being the confocal parameter.

By analogy with (1), the vector field $\mathbf{E}_0(x_0,y_0,0)$ can be represented as a series of Hermite-Gaussian functions [8, 26–28]; for the sake of simplicity, we will confine ourselves to considering one polarization component and omit index notations:

$$E_x(x_0,y_0,0)=\sum_{n,m}^{\infty}\frac{A_{n,m}\sqrt{2}}{\sqrt{w_0^2\pi 2^{m+n}m!n!}}\,\Phi_n\left(\frac{\sqrt{2}x_0}{w_0}\right)\Phi_m\left(\frac{\sqrt{2}y_0}{w_0}\right). \qquad (8)$$

The coefficients $A_{n,m}$ are defined by the formula

$$A_{n,m}=\frac{\sqrt{2}}{\sqrt{w_0^2\pi 2^{m+n}m!n!}}\int_{-\infty}^{\infty}\int_{-\infty}^{\infty}E_0(x_0,y_0)\times\Phi\left(\frac{\sqrt{2}x_0}{w_0}\right)\Phi_m\left(\frac{\sqrt{2}y_0}{w_0}\right)\mathrm{d}x_0\,\mathrm{d}y_0, \qquad (9)$$

and the field at an arbitrary plane z may be written as

$$E(x,y,z)=\sum_{n,m}^{\infty}A_{n,m}U_{n,m}(x,y,z). \qquad (10)$$

Hence, in the present case, the object transforms the principal mode $U_{0,0}(x,y)$ to the 'spectrum' $U_{n,m}(x,y)$ in indices m,n.

The field representation in the form of propagating non-uniform waves (6) is valid for limited index values. At large m,n, the transverse component of the wave vector exceeds $2\pi/\lambda$, and the amplitude decreases exponentially at finite distances z_n.

It is known from the theory of resonators [8, 25–27] that diffraction losses are largely dependent on the Fresnel number $N_{\rm F}=a^2/b\lambda$ and the fraction of the mode energy outside the mirror. In order to estimate superresolution and diffraction losses for higher-order modes, one needs to measure the effective mode radii $w_{n,m}$. In a symmetrical quasi-spherical resonator with distance between the mirrors $2F$, the size of the principal-mode spot in the plane $z=0$ at a sufficiently large magnification $M = W_0/w_0$ is [25]

$$w_0 \cong \frac{F\lambda}{\pi W_0} \, ,$$

where W_0 is the radius of the $\mathrm{TEM}_{0,0}$ mode at the mirror. The waist radius w_0 for $W_0 \cong a$ is approximately half as small as the radius of the Airy disk d_{R}, which is universally accepted to be the resolution criterion.

Let us consider a simple two-mode model [12] and show that limited information on the coordinates of the boundaries of a subwavelength structure $x_{1,2} = \pm d/2$ can be transmitted, under certain conditions, with a phase image in the form of π-jumps of the phase. In the one-dimensional case for the field portrait given by

$$E_0(x) = U_0(x) + a_2 U_2(x) = \frac{\sqrt{2/\pi}}{w_0} \exp\left(-\frac{x^2}{w_0^2}\right) \times \left\{1 + \frac{a_2}{\sqrt{2}}\left[\frac{4x^2}{w_0^2} - 1\right] \exp(2\mathrm{j}\phi)\right\}, \qquad (11)$$

the distance d between zero-lines is a function of the amplitude a_2

$$\frac{d}{w_0} = \left[1 - \frac{\sqrt{2}}{a_2}\right]^{1/2} .$$

Let us assume that the optical system does not introduce any amplitude-phase distortions into the field portrait $E_0(x)$. Then, in the image plane z_{i} conjugate to $z = 0$, where $\phi = \arctan z_i/b = 0$, the normalized distance $D_i/W_i = d/w_0$ remains unaltered and can be measured at a sufficiently large magnification, when $D_i \gg \lambda$. In the case of defocusing or phase distortion, when $\phi \neq 0$, the field has a finite minimum value in the vicinity of $x_{1,2} = \pm d/2$, and the coordinates are complex quantities. As the field $E_0(x)$ intersects the zero-line $x_{1,2}$, its phase experiences a π-jump, which can be interpreted as the intersection of the wave front dislocation line near which there is a large phase gradient.

It follows from this isolated example that limited information on a subwavelength structure can be obtained even with a small increase in the number of internal degrees of freedom for the field. Also, this simple example may be used to illustrate a marked difference between the phase-related and amplitude-related information derived from the field portrait (11) and the effects of energy relationships between field components. The amplitude contrast in the vicinity of $x = 0$ falls off as squared d/w_0 as the distance d decreases, whereas π-jumps in $\arg E_0(x)$ occur at any d/w_0 value. Let us further assume that the normalized amplitude a_2 in the image plane proved to be smaller than the critical value $\sqrt{2}$ due to the increase of diffraction lasses with increasing the mode index. In this case, information concerning zero-lines is totally lost in the field portrait.

Let us now consider a more general case of an unlimited number of modes and find the dependence of the waist effective radii w_n of higher-order modes on a single mode index n. The effective radius w_n of an even nth mode is defined by the condition

$$\frac{\Phi_n(w_n)}{\Phi_n(0)} = \frac{H_n(w_n)}{H_n(0)} \exp\left[-\left(\frac{w_n}{w_0}\right)^2\right] = \mathrm{e}^{-1} \, . \qquad (12)$$

At small n, the plots of functions Φ_n presented in [25, 27] may be used for the numerical evaluation of w_n. At large n, the representation [8] of the Hermite polynomials as a series in powers of $t = \sqrt{2} w_n/w_0 = \sqrt{2} G_n$, i.e.,

$$H_n(t) = 2^n t^n - 2^{n-1}\binom{n}{2} t^{n-2} + \ldots \, , \qquad (13)$$

$$H_n(0) \cong 2^{n/2}(n!)^{1/2} \, ,$$

is suitable for the same purpose.

If the indices n and the normalized mode radii in the series (13) are sufficiently large ($G_n \gg 1$), it is possible to use only the first term; in such an approximation, $G_n(n)$ is implicitly defined by the equation

$$1.2n - \frac{n}{2}\ln n + n \ln G_n - G_n^2 + 0.54 = 0 \, . \qquad (14)$$

The G_n dependence on n is plotted in Fig. 2. The dashed line shows its approximation by the function $G_n \cong n^{1/2}$.

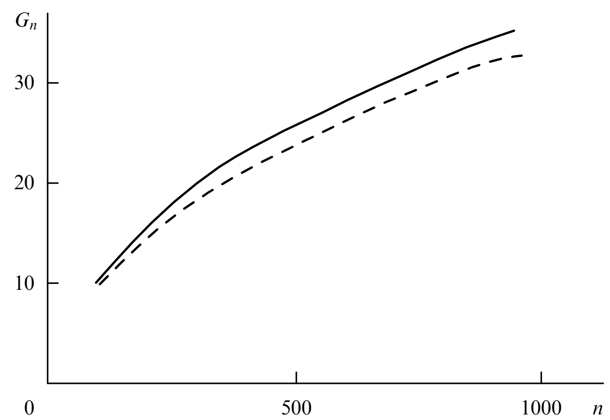

Figure 2. Dependence of the normalized radius of the nth mode $G_n = w_n/w_0$ on index n. Dashed line shows approximation by the function $G_n = \sqrt{n}$.

Let us now consider spatial variation of modes with large indices n, paying special attention to the following feature essential for the final conclusion. In the fixed cross section $z = 0$, a rise in n entails the growth of w_n concomitant with a slow decrease in the mean distance between the adjacent zeros of the $\Phi_n(\sqrt{2}x/w_0)$ function along the coordinate x. Figure 3 shows, for the sake of illustration, the plots for $n = 0, 2, 12$ borrowed from [27], which demonstrate an approximately twofold fall in the period D_{12} of the function Φ_{12} as compared with D_2. Naturally, the functions $\Phi_n(\sqrt{2}x/w_0)$ are not strictly periodical in the interval $\pm w_n$, but this aperiodicity becomes immaterial at high n.

The number of zeros of the function $\Phi_n(\sqrt{2}x/w_0)$ in the interval $2w_n$ is n, and the mean value of the half-period D_n at large n is $D_n = 2w_n/n$. Let us denote the number of zeros in the interval $-w_0 \leqslant x \leqslant +w_0$ as $S(n)$, assuming their distribution to be uniform.

This yields, for the number of zeros or half-periods $S(n)$ of the function $\Phi_n(\sqrt{2}x/w_0)$ within the diameter $2w_0$ in the same approximation,

$$S(n) \cong \frac{n}{G_n} \cong n^{1/2} \cong G_n \, . \qquad (15)$$

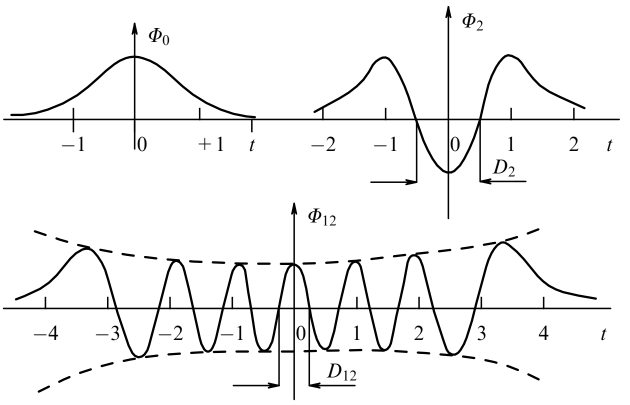

Figure 3. Hermite-Gaussian functions with $n = 0, 2, 12$. It is seen that, with increasing n and decreasing D_n, the functions behave quasi-perodically within the interval $-1 \leqslant t \leqslant 1$.

The functions

$$\Phi_s\left(\frac{\sqrt{2}x}{w_0}\right) \cong \left\{ \begin{array}{c} \sin\left(\dfrac{s\pi x}{w_0}\right) \\ \cos\left(\dfrac{s\pi x}{w_0}\right) \end{array} \right\} \tag{16a}$$

at $S(n) = 0, 1, 2, \ldots, S(n_{\max})$ and the appropriate renormalization may be regarded as a new basis of a finite dimensionality. In this basis, the field

$$E_s(x) = \sum_{s=0}^{S} A_s \Phi_s(x) \tag{16b}$$

can be represented in the interval $-w_0 < x < +w_0$ by a series in functions (16a); in this series, s has the sense of the index of eigenfunctions $\Phi_s(x)$ within the waist diameter of the zeroth mode ($2w_0$). It follows from (15) that $s = n^{1/2}$, and only a limited number of modes in the series (10) make contribution to $E_s(x)$. This line of reasoning suggests the possibility of the existence of a limited basis (16a) in the complete set of functions (10) necessary for the representation of the field inside the zero-mode waist.

Also, the number $S(n_{\max}) \cong G_n(n_{\max})$ may be interpreted as a superresolution parameter or the number of 'internal' degrees of freedom of a field, because it defines the minimum half-period D_n

$$D_n = 2G_n \frac{w_0}{n} \cong \frac{2w_0}{G_n(n_{\max})} \,. \tag{17}$$

The same refers to the field distribution along the coordinate y, and the total maximum number of the 'internal' degrees of freedom is

$$G^2(n_{\max}) \cong n_{\max} \,.$$

Eqn (17) may be used to estimate the value of z_n at which the equality $D_n(z_n) = 2z_n \lambda n^{-1/2}(\pi w_0)^{-1} = \lambda/2$ is fulfilled. The interval z_n, in which the amplitude decreases exponentially increases with increasing mode index:

$$z_n \cong \frac{\pi w_0 n^{1/2}}{4} \cong \frac{\lambda n^{1/2}}{4NA} \,.$$

Variation of the amplitude in this interval is defined by an exponent with index $\pi z/D_n(z) \cong \pi w_0 n^{1/2}/2\lambda \cong n^{1/2}/2NA$.

Figure 2 shows that a 10-fold superresolution can be obtained if the image contains approximately 100 modes along a single coordinate, with the mode radius w_{100} being only 10 times that of the radius w_0.

Qualitative estimates in the above formulas should be treated with caution because of the aforementioned disagreement with the paraxial approximation and the assumptions adopted without estimates. We believe, however, that the main qualitative relationships and conclusions will remain valid after a more accurate analysis.

Putting aside for a while the interpretation of the function $S(n_{\max})$ as the number of internal degrees of freedom, we will focus on the diffraction losses, which determine the number of effective modes $0 < n < n_{\max}$ and the largest radius of the meaningful mode $W_n \leqslant W_{n_{\max}}$ at the exit from an optical system. A substantial difference between the series (2a) and (16b) lies in the criteria for the truncation of the expansion.

A rough estimate of $S(n_{\max})$ is possible based on the equality of the nth-mode radius in the lens plane to the lens' radius $W_{n_{\max}} = a$. Bearing in mind that $w_0 = \lambda F/\pi W_0$, we have

$$S(n_{\max}) \cong \frac{a}{W_0} = N_{\mathrm{F}}^{1/2}\left(\frac{\pi w_0}{\sqrt{\lambda F}}\right) \cong N_{\mathrm{F}}^{1/2}\sqrt{\frac{\pi}{M}} \,. \tag{18}$$

It follows from (18) that $n_{\max}$ naturally increases with the Fresnel number N_{F}.

It is possible to obtain a more exact dependence of $n_{\max}$ on the system's parameters taking into account the relationship between complex amplitudes $A_{n,m}$ and $B_{n,m}$ inside and at the outlet of an open resonator, respectively [8, 27, 28]:

$$\bar{B}_{n,m} = \bar{A}_{n,m} \exp(-\mathrm{j}\alpha - \beta) \,. \tag{19}$$

The functions $\alpha(N_{\mathrm{F}}, n, m)$ and $\beta(N_{\mathrm{F}}, n, m)$ increase with growing n, m and describe the amplitude and phase distortions introduced by the lens in the image field $\mathbf{E}(x, y)$. The corresponding permissible levels $\alpha \leqslant \hat{\alpha}$, $\beta \leqslant \hat{\beta}$ can be found experimentally or by calculation. If $\hat{\beta} < \hat{\alpha}$, the indices first become restricted in phase and then in amplitude, which leads to the prevalence of phase distortions over amplitude ones in the image.

The absence of modes with $n \geqslant n_{\max}$ in the image results in the limited superresolution $S(n_{\max})$. In order to qualitatively estimate the effect of optical system parameters on $S(n_{\max})$, we must know the behavior of losses at large index values. Unfortunately, we do not have analytical dependences of losses on mode indices for nonconfocal resonators, and they can be obtained only in an indirect manner.

The configuration for $W_0 \gg w_0$ given in Fig. 1b resembles that of a hemispherical resonator, which makes it possible to use the formulas of L A Vainshtein [8, 27, 28] for plane-parallel resonators with round mirrors

$$\alpha_{l,p} = \frac{8k_{l,p}^2 \delta(m+\delta)}{\left[(m+\delta)^2 + \delta^2\right]^2} \,, \qquad \beta_{l,p} = \frac{m}{4\delta}\,\alpha_{l,p} \,, \tag{20}$$

where $m = (8\pi N_{\mathrm{F}})^{1/2}$, $\delta = 0.84$, and $k_{l,p}$ is the pth root of the lth-order Bessel function.

In the case of confocal configuration, one may also use Slepyan's formulas given in [8]

$$\alpha_{l,p} = \frac{2\pi(8\pi N_{\mathrm{F}})^{2p+l+1}\exp(-4\pi N_{\mathrm{F}})}{p!(p+l)!}\,,$$
$$\beta_{l,p} = (2p+l+1)\,\alpha_{l,p}\,\frac{\pi}{2}\,. \tag{21}$$

Hereafter, we will ignore the difference between indices n, m and p, l despite the fact that the radial and azimuthal indices in the cylindrical system of coordinates are not equivalent.

Note that in this case formulas (21) overestimate indices $p(N_{\mathrm{F}})$ as compared with (20). It appears from these formulas that phase distortions prevail over amplitude ones; therefore, maximum values of indices for a given level of distortions should be estimated in terms of phase. Numerical calculations indicate that at $l = 0$ and $p \gg 1$, dependences $p_{\max}(N_{\mathrm{F}})$ for (20) and (21) are rather well approximated by the expressions

$$p_{\max} = 0.4N_{\mathrm{F}} \tag{22a}$$

and

$$p_{\max} = 5N_{\mathrm{F}}\,. \tag{22b}$$

The difference between the coefficients is related to the fact that losses in a confocal resonator are smaller by an order of magnitude than those in a resonator with flat mirrors.

The use of the approximation $S = n^{1/2}$ and the assumption that $n = p$ lead to a simple dependence of the limiting superresolution on the Fresnel number

$$S_p(N_{\mathrm{F}}) = (CN_{\mathrm{F}})^{1/2}\,, \tag{23}$$

where $C \approx 0.4-5$. The corresponding graphs are shown in Fig. 4.

To obtain $S = 10$, it suffices that N_{F} be equal to 250, which gives, at $NA = 1$ and $\lambda = 633$ nm, realistic values for the entrance aperture diameter $2a = 0.32$ nm.

Let us now consider the effect of defocusing on superresolution, because this may be one more cause for the disturbance of phase relations between modes.

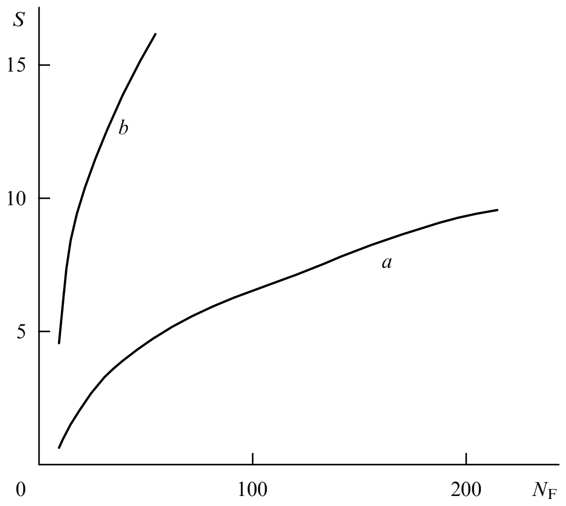

Figure 4. Plots of limiting superresolution vs the Fresnel number: (a) from the Vainshtein formula [28]; (b) from the Slepyan formula [8].

Indeed, it follows from (7) that the dependence of the phase of the n, m-mode on the axial coordinate z grows with n, m:

$$\varphi(z) = (m+n+1)\arctan\frac{z}{b}\,.$$

The phase shift of the n, m-mode relative to the zeroth mode

$$\mathrm{d}\varphi_{n,m} = \varphi_{n,m} - \varphi_{0,0} = (m+n)\arctan\frac{z}{b} \tag{24}$$

vanishes only in the conjugate waist planes $z = 0$ and $z = z_{\mathrm{i}}$. A change in the sign of the object's plane displacement dz relative to the focal plane entails a change in the sign of the phase difference $\mathrm{d}\varphi_{m,n}$, which can be visually perceived as the inversion of the phase image.

The equivalent confocal parameter b for a concentric resonator is close to zero. Therefore, $\mathrm{d}\varphi_{m,n}$ asymptotically approximates $(n+m)\pi/2$ at relatively large defocusings $(z \gg b)$. The initial amplitude–phase relationship needs to be retained if an image is to be adequately reproduced. For this reason, the requirements for the quality of objectives and the accuracy of focusing grow with increasing n, m. It is easy to see that in the case of defocusing within the standard depth of focus $\mathrm{d}z \cong \lambda/2(NA)^2$, phase shifts considerably exceed π.

Let us now turn to the concept of the degrees of freedom for the field in an image, which is crucial for good understanding of the problem in question.

In the Abbe diffraction theory of optical images [7, 8], the number of independent elements q is equal to the ratio of the linear field size to the Airy disk radius. In our model presented in Fig. 1b, the axis z of an equivalent resonator defines the position of the center of the zero-mode Gaussian beams. At first sight, this model contains a preferred axis, at variance with the known requirement [7] that an optical system should be isoplanar. However, at a large magnification $(W_0 \gg w_0)$, the configuration of an equivalent resonator resembles that of a concentric one, in which the position of the optical axis is less determinate. It is quite natural that a displacement of point x relative to the optical axis in the lens plane results in an additional restriction upon the maximum radius $W_n \cong a - x$, and, hence, on the spatial resolution which linearly decreases as the edge is approached. This fact allows the above discrepancy to be partly eliminated and the data obtained to be interpreted in the following way.

Suppose that the concentric resonator in Fig. 1b has $q^2 = q_x q_y$ independent zeroth modes $\Phi_{0,v}(x)$, $\Phi_{0,u}(y)$ with $v, u \leqslant q$ that are analogs of the angular prolate-spheroidal functions [8] with differently oriented wave vectors $\mathbf{k}_{v,u}$ within the solid angle $(a/F)^2$.

From this point of view, the series

$$\mathbf{E}(x,y) = \sum_{v,u}^{q} \mathbf{B}_{0,0,v,u}\Phi_{0,v}(x)\,\Phi_{0,u}(y) \tag{25}$$

may be interpreted [8] as the expansion of the function $E(x,y)$ in the zeroth modes in Gilbert space where the functions $\Phi_{0,v,u}(x,y,z)$ of the 'external' degrees of freedom form the basis. The space dimensionality is q^2, i.e., the number of external degrees of freedom.

For each of the q states of field (25), there is a finite subset $S(n)^2 \cong n_{\max}$ of effective internal degrees of freedom related, for example, to the higher-order modes $\Phi_s(x,y)$ (15). They form a finite-dimensional Gilbert subspace in the basis $\Phi_{n,m}$, with the number of degrees of freedom for each coordinate being determined by the Fresnel number N_F of the optical aperture (see graphs in Fig. 4).

We believe that the most important result of the above analysis is the presence of propagating high-order modes in the field portrait, which allows, in principle, the number of the degrees of freedom of an image to be increased. Another important finding is a much broader range of transmitted spatial frequencies in the case of correct interpretation of the effect of the entrance aperture. The field representation in the basis of an optical system serves to explain, in the two-mode model approximation, the transmission of minimal information on a subwavelength field portrait and demonstrates the effect of amplitude and phase distortions. The quasi-periodicity of the high-order Hermite-Gaussian functions provides formal grounds for the representation of internal degrees of freedom of a filed.

However, the proposed physical concept, not confirmed by consistent computation, has important aspects worthy of special analysis in the future.

To begin with, one must be certain that the obtaining of exact solutions for the eigenfunctions does not introduce substantial corrections into the results obtained in previous paragraphs. Naturally, the energy contribution of higher-order components to (25) decreases with increasing index. Therefore, one of the conditions for the realization of superresolution is the discrimination between weak components and relatively intense low-order modes in the image field. With the contrast enhancement technique, this is achieved by compensating for the background and broadening the dynamic range of image brightness, and in computer phase-contrast microscopy, by measuring local phase values of the low-intensity interference field. Also, it is worth noting that the use of higher-order modes makes it possible to obviate the fundamental near-field problem and account for the transmission of information on the higher spectral components in the field portrait which formally correspond to exponentially decaying plane waves with $D_n \ll \lambda$.

3. Measurements with a computerized Airyscan phase microscope

The optical arrangement of the computer-aided phase-contrast microscope Airyscan [29] is based on the modified scheme of a Linnik-type interferometer with phase modulation of the reference wave. The light source is an He-Ne laser ($\lambda = 633$ nm), local values of the interference signal phase are measured with a coordinate-sensitive detector (image dissector and analog-to-digital converter). The software enabled an operator to obtain pseudocolored topographs, cross sections, and three-dimensional images, to carry out statistical analysis using standard program packets, to record dynamic processes at arbitrary points, to perform their Fourier analysis, etc. The block diagram of the instrument is shown in Fig. 5, where *1* is the zero-mode He-Ne laser, *2* is the beam-splitter, *3* is the reflecting object, *4* is the reference mirror with a piezotransducer, and *5* is the dissector image tube.

Field sizes were calibrated against certified diffraction gratings with a 0.85-μm spacing. Interchangeable 10 to 100× objectives were used, but most measurements were performed using a Zeiss 100/0.9 objective. The general optical magnification achieved with the microscope was 3.500×, and zooming allowed 300×300-nm image fragments to be distinguished with a minimal pixel size of 3 nm.

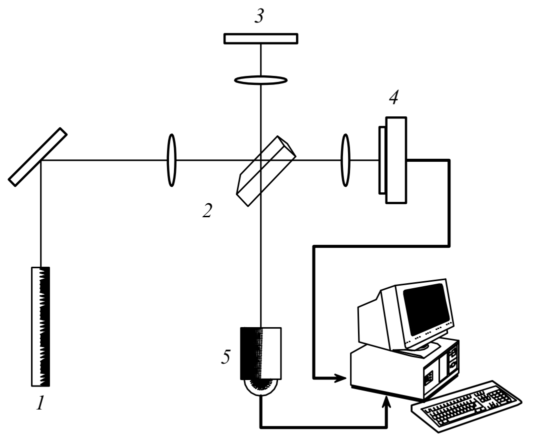

Figure 5. Optical scheme of a computer-aided Airyscan phase-contrast micrscope [29]: *1*, zero-mode He-Ne laser; *2*, beam-splitter; *3*, object; *4*, reference mirror with a piezotransducer; and *5*, dissector image tube.

We present here new data obtained by G E Kufal' with a view to reveal major factors affecting superresolution. More detailed data on measuring objects of different nature can be found in [29 – 33]; in some cases, they confirmed good correspondence between an object and its image for structures 100 – 2000 nm in size.

The identification of a phase image with the real structure was greatly facilitated in the case of its large size and in the presence of an *a priori* information. For example, measurements of the profile of optically inhomogeneous phase-shifting Levenson-type masks [34] yielded reliable data notwithstanding their complicated structure. These results confirmed that computer-aided phase-contrast microscopes are equally promising for monitoring semiconductor integrated circuits [30] and measuring submicron line widths.

Examination of virtually any polished reflecting surface with the Airyscan microscope revealed traces of its mechanical treatment, microinclusions, and defects with linear sizes of a few microns. Zooming fragments in the images allowed progressively smaller structures to be detected, e.g., extended structures measured only few tens of nanometers were in many cases found in the linear fragments of 200 – 300 nm in size.

It proved far more difficult to interpret images of biological objects, which required even more professional skill and a priori information. Nevertheless, plant cells were found to show a contrast nucleus, walls, and mitochondria. Cell images of fungus *Corioulus hirzurus* exhibited a protein/lipid bilayer in the walls with a width of individual layers of 50 and 80 nm [31]. Also, chromatin distribution in *E. coli* was studied.

Figure 6a presents a topograph of a smallpox vaccine containing virus particles about 400 nm in transverse diameter. Note also characteristic subunits with an apparent size of about 30 nm.

Figure 6b shows the cross-sectional profile of *Rickettsia provazekii* which confirms the possibility of recording contrast elements of biological structures with a 220-nm difference in the equivalent height and a linear size of less than 50 nm. Under certain conditions, images contained prominent artifacts in the form of characteristic concentric rings due to light speckles and interference; these features, however were

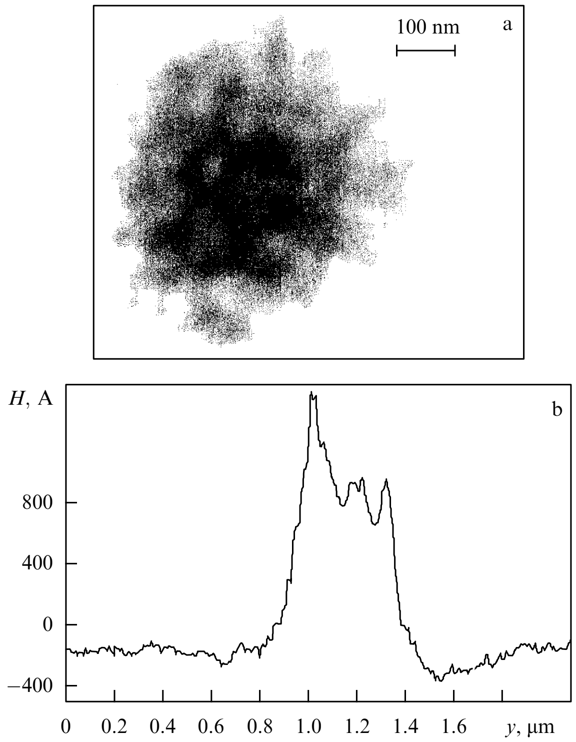

Figure 6. (a) Topograph of a smallpox virus vaccine (phase-contrast image). (b) Cross-sectional profile of *Rickettsia provazekii*.

markedly different from the structures shown in Fig. 6a in the shape, size, and equivalent height.

The images were highly susceptible to accurate focusing which was a minor fraction of the nominal depth of focus $dz = \lambda/2[NA]^2$ [7].

Of special interest are the results of measuring latex spheres which are frequently used as test structures. Latex suspensions with particles of 50, 110, 260, 630, and 920 nm in diameter were applied on a substrate of polished silicon or aluminum (note that surface finish had marked effect on the profile of interest). The measured dimensions were close to the real ones in the case of large particle diameter (920 and 630 nm) in suspensions applied on aluminum. Deviations increased with decreasing particle diameter and were close to the asymptotic limit at 300 nm. The results were even more accurate for spheres of small diameter on a silicon substrate, with the limit of 500 nm. Isolated 50 – 110-nm spheres were readily distinguishable, but their measured size was usually overestimated. The topographs exhibited spheres of apparently pseudoelliptic shapes with axial ratios of 0.7 – 0.9, spreading in the direction of the polarization plane.

The results of these measurements confirm the importance of examining the 'field portrait' for a certain class of models, including dielectric spheres with small refractive index.

Diffraction-grating images displayed the following specific features: maximum contrast at H-polarization of the incident wave, impaired contrast of the profile image with decreasing grating spacing, and the lack of significance for the measurements of gratings with the number of lines over 1800/mm; the minimally discernible spacing in a periodical structure (*ca* 400 nm) exceeded greatly the minimal width (50 – 100 nm) resolvable for single slits.

Profile measurements using certified sandwich structures with a slit width of 50 – 400 nm [5] were particularly demonstrative. The height difference was normally not more than 200 nm, although the slit depth exceeded 2 μm. With decreasing width, the effect of artifacts increased and the results of measurements were lacking in significance. Structures with a determinate profile displayed inversion of contrast as the object's surface moved relative to the focal plane. This finding is in qualitative agreement with (24).

Images of stepwise structures at $dh \cong \lambda/4$ showed slope widths of several nanometers, but these figures do not reflect the real resolving power of the microscope.

Of course, all these findings are insufficient to comprehensively describe the properties of phase-contrast images of subwavelength structures. However, taken together with the results of previous studies [1 – 6, 21 – 24, 30 – 33], they provide enough material for the following general conclusions:

1. Superresolution is possible for both conventional amplitude images and phase-contrast images under coherent illumination. A specific feature of phase images is the separation of information on the local distribution and anisotropy of the refractive index, in conjunction with the reliable identification of the boundaries of contrast structural elements, to which minimal field intensities correspond.

2. Marked superresolution is attainable only with large numerical apertures of the objectives and at high magnifications.

3. Using standard structures with clear-cut edges, good correspondence between an object and its phase image can be achieved when the superresolution parameter is $S = 2$–6.

4. Superresolution of up to $S = 20$ is possible in images of unidentified structures, but their profiles are highly susceptible to careful focusing.

5. Polarization dependence of phase images is largely a function of the 'field-portrait' properties of real objects.

6. The resolution in images of isolated structures is higher than in periodic ones.

7. Characteristic artifacts in phase images can be seen as apparent breaks of the surface related to wave-front dislocations and phase uncertainty [12]. A displacement of an object relative to the focal plane may lead to profile inversion, local profile distortions caused by coherent noise, and speckle structures due to reflections in the optical system and apparent contrast enhancement at local height differences close to $\lambda/4$. A priori information is necessary for the correct interpretation of images.

8. The distance between boundary lines where the optical parameters and the profile height of independently certified test structures with high reflection coefficient undergo a sharp change may serve as a criterion for the resolution in phase images. Normalized superresolution S may be defined as the ratio of the Airy disk radius to the minimal measured distance between the contrast boundary lines of extended structural elements.

4. Conclusions

The present review and the previously published literature demonstrate the possibility of superresolution in phase images.

The data available disagree with the Abbe diffraction theory [7, 8] in which the effect of the aperture reduces to the restriction of the angular spectrum. The aim of the present report is to explain this discrepancy. The most essential features in this context are the use of eigenfunctions of an optical system as the basis, the calculation of diffraction losses taken from the theory of open resonators, the extension of the concept of the degrees of freedom of an image to the Airy disk, and the consideration of the 'field portrait' of a subwavelength structure as a separate problem.

It appears appropriate to remind that the Kirchhoff theory [7, 8, 26] implies the smallness of the numerical aperture and represents the phase in diffraction integrals as a power series in transverse coordinates in which the second and third terms describe the Fraunhofer and Fresnel diffraction, respectively, whereas higher-order terms are neglected. The object's field is represented by a series in plane waves, and components with imaginary negative values of the wave number (to which evanescent waves formally correspond) are normally assumed [8] to make no contribution to the image.

The Fresnel approximation is employed in the Fredholm integral equation to calculate eigenfunctions of an open resonator, which leads, in the paraxial approximation, to the Hermite-Gaussian functions. In this case, however, the lack of exact solutions for large Fresnel numbers does not hamper the formal field representation in the basis of eigenfunctions, and the use of solutions in the paraxial approximation reveals a number of regular features in higher-order modes. We think that exact solutions will confirm the diffraction limitation on the maximum mode index and the dependence of their complex amplitude on the Fresnel numbers of the mirrors; then, the disagreement with the results of analysis described earlier in this paper will primarily affect numerical estimates. A decrease in the quasi-period D_n with increasing index of transverse modes and the existence of solutions at $D_n \ll \lambda$ allows the conflict with the classical image theory (in which they are identified with non-propagating waves) to be eliminated and ensures qualitative agreement with experimental findings.

A formal sequel to the proposed concept is the representation (10) of the object's field as a series in Hermite-Gaussian modes with the unlimited transverse index, which is equivalent to the cancellation of the restriction on the spatial frequency spectrum of the field portrait, the description of diffraction at the aperture by the amplitude-phase distortion function (19), the evaluation of the number of effective modes in an image, the introduction of the concept of the internal degrees of freedom of an image, and the explanation of some regular features in the experimentally observed superresolution. The most important of these features are the dependence of superresolution on the Fresnel number for the entrance aperture, a rise in sensitivity to focusing with decreasing linear size, and phase inversion in the vicinity of $z = 0$.

The impaired correspondence between the image and the 'field portrait' is the inevitable payment for the superresolution.

When the present work had already been prepared for publication, we read a review of H G Schmidt-Weinmar [35] devoted to a broader problem of reconstructing source fields with the subwavelength spatial resolution based on optical measurements in the far field; reading through this review allowed a few corrections to be introduced into the proposed concept. The review [35] is not directly concerned with microscopy and effects of the entrance aperture but contains an analysis of studies relevant to the general theory of propagation of electromagnetic waves reported by A Sommerfeld, C J Bouwckamp, H Kasimir, G Herzle, and N Trulley whose results can be used to develop a new approach to the explanation of superresolution in microscopy.

Here are the findings of primary importance for our purpose.

The field of a source may be represented by non-uniform multipole waves to which a complex two-dimensional spectrum of spatial frequencies corresponds. Information available in the far field is contained in the spectrum of uniform plane waves, and the superresolution is related to non-uniform waves of higher orders. Two groups of functions may be arbitrarily distinguished in the basis of the source-field representation. Propagating waves and the classical resolution limit are related to lower-order functions, while essentially non-uniform waves decaying in the direction of their propagation correspond to higher-order functions. They are able to transmit limited information on the more intricate structure of a source within a given wavelength. Multipole fields are characterized by the power-like dependence of the rate of amplitude decay down to a certain distance ('barrier' width) at which the spatial period in the transverse plane is smaller than the wavelength. Behind the 'barrier,' whose width is proportional to the order of multipole, the amplitudes decrease as $1/r$. In the framework of this model, it is possible to estimate the number of effective modes contributing to the image.

The text book by A Siegman [36] reports a formula for the mean period of the Hermite–Gaussian function at large indices and the effective radius coincident with the formula (15) in our review.

Acknowledgments. This work was supported by the Russian Foundation for Basic Research (grant 95-02-05178-a).

The author is grateful to G E Kufal' for fruitful cooperation in the improvement of the Airyscan microscope and the participation in experimental studies. Useful discussion of theoretical aspects with Professor Yu A Kravtsov and V P Bykov and their critical comments enlightened me on a number of important problems. Personal contacts with Dr. M Totzeck and information on the results of his work were very helpful.

The author is indebted to professor V I Shmal'gauzen for helpful discussion and comments.

References

1. Allen R D, Allen N S, Travis J L *Cell Motility* **1** 291 (1981)
2. Weiss D G, Maile W, in *Electronic Light Microscopy* (New York: Wiley-Liss, 1993) p. 105
3. Inoue S *Video Microscopy* (New York: Plenum, 1986)
4. Tychinsky V P *Opt. Commun.* **74** (1–2) 41 (1989)
5. Tychinsky V P et al. *Pis'ma Zh. Tekh. Fiz.* **17** (22) 80 (1991)
6. Tychinsky V P *Proc. SPIE Conf.* **1464** 80 (1992)
7. Born M, Wolf E *Principles of Optics* 2d edition (Oxford: Pergamon, 1970) [Translated into Russian (Moscow: Nauka, 1970)]
8. Solimeno S, Crosignani B, Di Porto P *Guiding, Diffraction and Conntrinement of Optical Radiation* (Orlando: Academic Press, 1986) [Translated into Russian (Moscow: Mir, 1989)]
9. Toraldo di Francia G *Nuovo Cimento, Suppl.* **9** 426 (1952)
10. Tychinsky V P, Velzel C H F, in *Current Trends in Optics* (Ed J C Dainty) (London: Academic Press,1994) p. 255
11. Pask C *J. Opt. Soc. Am.* **66** 68 (1976)
12. Tychinsky V P *Opt. Commun.* **81** 131 (1991)
13. Ash E A, Nicholls G *Nature* (London) **237** 510 (1972)
14. Lewis Aaron, in *Current Trends in Optics* (Ed J C Dainty) (London: Academic Press,1994) p. 233
15. Vigoureux J M, Depasse F, Girard C *Appl. Opt.* **31** (16) 3036 (1992)

16. Wyant J C, Creath K *Laser Focus/Electro-Opt.* **21** (11) 118 (1985)
17. Creath K *Proc. SPIE Conf.* **1464** 474 (1991)
18. Creath K *Proc. SPIE Conf.* **1319** (1990)
19. Pommet D A, Moharam M G, Grann E B *J. Opt. Soc. Am.* **11** (6) 1827 (1994)
20. Pasman J, in *Principles of Optical Disc System, International Trends in Optics* (Ed. A Hilher) (Bristol: LTD, 1991)
21. Totzeck M *J. Eur. Opt. Soc., P.A: Pure Appl. Opt.* **3** 867 (1994)
22. Totzeck M, Krumbugel M A *Opt. Commun.* **112** 189 (1994)
23. Nyyssonen D, Seligson J, Masor I *Proc. SPIE Conf.* **1926** 299 (1992)
24. Davidson M P, Monahan K M, Monteverde R J *Proc. SPIE Conf.* **1464** 155 (1991)
25. Haus H A *Waves and Fields in Optoelectronics* (Englewood Cliffs: Prentice-Hall, 1984) [Translated into Russian (Moscow: Mir, 1988)]
26. Maitland A, Dunn M H *Laser Physics* (Amsterdam: North- Holland, 1969) [Translated into Russian (Moscow: Nauka, 1978)]
27. Anan'ev Yu A *Opticheskie rezonatory i problema raskhodimosti lazernogo izlucheniya* (Optical Resonators and the Problem of Laser Radiation Divergence) (Moscow: Nauka, 1979)
28. Vainshtein L A *Otkrytye rezonatory i otkrytye volnovody* (Open Resonators and Open Waveguides) (Moscow: Sov. radio, 1966)
29. Tychinsky V P et al. *Opt. Commun.* **74** (1–2) 37 (1989)
30. Tychinsky V, Tavrov A *Proc. SPIE Conf.* **1673** 483 (1992)
31. Reshetnikova I A et al. *Mikrobiologiya* **61** 5 880 (1992)
32. Tychinsky V P, Tavrov A, Shepelsky D *Proc. SPIE Conf.* **1647** 96 (1992)
33. Tychinsky V P et al. *Proc. SPIE Conf.* **2329** (1994)
34. Levenson M D *Physics Today* **July** 28 (1993)
35. Schmidt–Weinmar H G, in *Inverse Sourse Problems in Optics* (Ed H P Baltes) (New York: Springer, 1978) p. 143
36. Siegman A E *Lasers* (Mill Valley, Cal.: Univ. Science Books, 1986)